# Planning and Control of Anthropomorphic Robotic Hands using Synergies

Marco Henriques

***Abstract*— In this work we present a method for the generation of hand postural synergies for a series of precision grasp types to be used in dextrous robot hands. Our method records the robot hand motions while teleoperated by human subjects via a dataglove, doing different grasp types on a series of objects. This exploits the fact that humans automatically compensate for calibration errors on the glove to robot mapping. The method is applied to the Shadow Robot Hand and to the iCub Hand. Despite the hands having a significantly different number of actuators, our analysis demonstrates that the effective number of degrees-of-freedom of the tested precision grasps is lower than the number of actuators in both hands. Therefore, the existing actuators are enough to drive the hands with realistic human-like postures and in-hand movements. In line with previous works on general grasp synergies, our work confirms that human precision grasps also lie on low-dimensional spaces.**

## I. INTRODUCTION

The capacity of the human hand to grasp and manipulate objects, known or unknown and of widely different sizes, shapes and materials is unmatched. Despite recent progress in the design and control of multi-finger robot hands, their use in service-robotics is still limited by the complexity of finding and applying grasp movements for a given task.

Two main approaches have been used to tackle the grasp-planning problem. In analytical approaches, a *grasp* is formally defined as a set of contact points on the surface of the target object together with friction cone conditions [1]. The traditional solution to this problem is divided into two stages: first, suitable grasping points on the object are determined, and in the second step a robot hand posture is computed via inverse kinematics to reach those points with the fingertips. See [2] and [3] for extensive reviews. Several contact models and grasp quality measures have been proposed to identify and evaluate different candidate grasps, and an elaborate theory of the kinematics and dynamics of finger and objects movements is available. Given the kinematics structure of a robot hand, any finger posture is fully specified by the joint angles, and can be thought of as a point in a high-dimensional joint space.

To realise a better flexibility and robustness, the second approach is motivated by the way humans grasp, and relies on empirical studies and classification of human manipulation tasks [4]. Typically, the manipulation task is divided into different phases, e.g. pre-shape, grasp, and stabilization of an object [5]. Analyzed human strategies can then be mapped to a robot hand, and complex behaviour is created by sequencing and combining basic motion primitives [6].

One key insight from research on human grasping is that most human grasp postures are derived from a small set of common pregrasp shapes. In their classical study, Santello et. al. [7] asked several test subjects to shape their hands as if to manipulate imaginary everyday objects, while the hand poses were recorded with a data-glove. The study clearly demonstrated that the fingers were shaped using certain patterns, or *grasp synergies*. A Principal Component Analysis of the recorded data showed that the two first principal components accounted for more than 80% of the variance, strongly suggesting that the grasp postures used by the humans could be approximated by a 2-dimensional basis instead of the 22-dimensional basis required to describe all 22 degrees-of-freedom typically assigned to the human hand. This fact is also reflected in the classical grasp taxonomies [4], where only a handful of different poses are sufficient to explain the hand motions used by humans for grasping.

Based on this idea, the concept of *eigengrasps* for robot hands for grasp-planning was introduced in [8]. The approach was refined in [9] and can dramatically reduce the effective dimension of the parameter space for grasp generation. Running the GraspIt! simulator [10] with this search technique, grasps could be generated quickly for thousands of 3D models, using a model of the human hand as well as different robotic hands. This collection of pre-calculated form closure grasps has been published as the Columbia Grasp Database [11]. The authors also suggest to use an object's 3D geometry as an index into the database, so that finding suitable grasps for a new object turns into a database lookup.

In this work we explore the use of grasp-synergies for planning and executing grasps with dexterous robot hands like the Shadow Hand and the iCub Hand. In contrast to previous works, we aim at the representation of precision grasps that can be used by the robotic platforms to execute in-hand manipulation tasks. We propose a teleoperation-based methodology for the acquisition of grasp data, where humans control the robot hand using a calibrated data-glove, while data is recorded directly from the robot joint angles. The key idea is that the human experimenters learn to compensate errors in the glove-to-robot map, thus bypassing the correspondence problem from the unknown hand kinematics of the experimenter to the kinematics of the robot. The recorded grasp datasets only include *human-like* grasps on the target objects, and it is then straightforward to calculate postural synergies for the robot. In our experiments, we recorded grasp data for eight different dexterous grasp classes, including pinch, tripod and lateral grasps. We show that a small number of parameters is sufficient to realise human like hand postures and movements. Some of the

derived synergy parameters are clearly related to meaningful grasping and object manipulation movements such as hand closure and in-hand rotations and translation, thus opening the way for novel planning and control algorithms.

The rest of this work is organized as follows. Section II provides a brief introduction to the topic of postural grasp synergies. It introduces the mathematical notation, the basic analysis and synthesis algorithms, and highlights the scope of our work. Section III describes our experimental setup. We introduce the main characteristics of the Shadow and iCub hands used in this study, presents the types of grasps and object set used in the experiments, and describes the experimental protocol. Section IV presents the results of our work, illustrating the performed synergy analysis and how they can be used in the control of the robot hands. Finally, Section V presents the main conclusions of this work and directions for future research.

## II. POSTURAL GRASP SYNERGIES

Postural grasp synergies are correlated configurations of the hand joints that typically occur during grasping tasks. For instance the hand closure movement typical in the reaching and pre-grasping phases of a manipulation task involves the synchronous contraction of the hand muscles so that finger and palm contacts with the object occur simultaneously. During this phase the fingers' joints assume postures that are highly correlated. In a robotic setting, let us define $\theta = \left[\theta^1, ..., \theta^N\right]^T$ the vector of joint angles[1], in a system with $N$ joints. We define a synergy $\mathbf{s_m}$ as a vector of weights $\mathbf{s_m} = \left[s_m^1, ..., s_m^N\right]^T$, where weight $s_m^n$ indicates how much joint $n$ should move under the activation of synergy $m$. This defines a linear model for the generation of hand postures as a function of a number $M$ of synergies and their corresponding amplitudes $\alpha_m$:

$$\theta = \mathbf{s_0} + \sum_{m=1}^{M} \alpha_m \mathbf{s_m} \tag{1}$$

where $\mathbf{s_0}$ is a nominal (or rest) hand posture. This can be written in matrix notation:

$$\theta = \mathbf{s_0} + S\alpha \tag{2}$$

where $S = [\mathbf{s_1} \mid \cdots \mid \mathbf{s_M}]$ and $\alpha = [\alpha_1 \mid \cdots \mid \alpha_M]^T$.

Synergies are related both to robot kinematics and task related aspects. Hand morphology, the arrangement of actuators and the typical grasping postures and objects have strong influence in the definition of the synergy vectors $\mathbf{s_m}$. A way to compute the synergy vectors from experimental data was proposed by [7]. This consists in computing the principal component analysis (PCA) of data vectors recorded in a large set of grasping trials. In that work data was acquired from humans shaping their hands so as to grasp imaginary objects while wearing a data-glove, a device that records the finger joint angles.

In our work, instead of recording data from the human hand angles, we acquire directly the values of the robot joints under teleoperation of the human subjects. Since we aim at using synergies for the control of the robot hands, recording the values from the robot angles provides us with a representation on the synergies that is directly mapped on the control space. Otherwise, we would have to map the human hand angles to robot angles which is a error prone procedure. Here we exploit the fact that humans, while tele operating the robot, receive direct visual feedback from the robot posture and can compensate mapping errors by performing small adjustments in their own hand shape so as to achieve the desired robot posture.

Once synergies have been defined or computed for a particular morphology and task, the generation of particular hand postures in a robot can be done by setting the contribution of each synergy to the overall posture through the weights $\alpha_i$ in Eq. (1). For instance, depending on the size of an object, the synergies correlated with hand closure should be activated accordingly. Depending on other object shape properties (flatness, roundness, etc) other synergy dimension should be activated. In fact, the analysis of [7] shows that the two main synergies are related to hand aperture and hand roundness/flatness, as these are the highest directions of variability in generic object grasping. However, as also noticed in that work, there are other directions that, despite smaller in variance, are significantly correlated with other object properties. In fact, object properties that are related to precision grasping are inevitably smaller in variance and thus get masked by the dominant motions, when a joint analysis is performed. In the contrary, in our work, we perform a segregated analysis of different types of precision grasps. An independent PCA analysis is performed for each one and stronger variances are observed for the first 5–6 synergies, thus supporting the empirical observations in [7].

### A. Synergy computation by PCA

In this section we describe the methodology to compute synergies from the principal component analysis of a data set of hand postures, either acquired from human finger angle measurements (as in [7]) or from the robots joints themselves (as in our case). Let the data vector extracted at trial $k$ be denoted $\theta_\mathbf{k}$. In a experiment with $K$ trials, the global mean is computed by:

$$\mathbf{s_0} = \frac{1}{K} \sum_{k=1}^{K} \theta_\mathbf{k} \tag{3}$$

The data vectors are subtracted from their mean, $\tilde{\theta}_\mathbf{k} = \theta_\mathbf{k} - \mathbf{s_0}$ and stacked in a data matrix $\Theta$:

$$\Theta = \left[\tilde{\theta}_\mathbf{1} \mid \cdots \mid \tilde{\theta}_\mathbf{K}\right]^T \tag{4}$$

Then the eigenvectors and eigenvalues of the data covariance matrix $R = \Theta\Theta^T$ reveals the most correlated directions in the joint space. The eigenvector decomposition can be performed by standard statistical analysis packages and computes the eigenvectors $\mathbf{e_i}$ and eigenvalues $\sigma_i^2$ such that:

$$R = E\Sigma E^T \tag{5}$$

[1]Symbol $T$ denotes the vector and matrix transpose operator.

with $E = [\mathbf{e}_1 \mid \cdots \mathbf{e}_n]$ and $\Sigma = diag(\sigma_1^2, \cdots, \sigma_n^2)$. The eigenvectors associated to the highest $M$ eigenvalues of $R$ are then defined as the synergy vectors. The selection of the number of synergies $M$ is usually made taken into account the amount of variance that is left out by not considering the lowest "energy" eigenvectors. Let us define the cumulative variance function as:

$$c(m) = \frac{\sum_{i=1}^{m} \sigma_i^2}{\sum_{i=1}^{N} \sigma_i^2} \times 100\% \quad (6)$$

The value of $M$ is typically chosen such as $c(M)$ takes about $80\%$ – $90\%$ of the overall variance.

### B. Precision Grasp Synergies

We perform independent statistical analysis for a selection of 8 precision grasp types from the taxonomy of [12]. A few human subjects tele operated the robot hands using a data-glove device in order to grasp different objects using each of the selected grasp types (see detail in Section III-D). Then, PCA analysis was performed for all the grasp trials of the same grasp type $g$, resulting in different synergy spaces $\{\mathbf{s_0^g}, S^g\}$. This allows to uncover some correlations between joints that are stronger than others for particular grasp types. The generation of instances of grasps is done according to Eq. (1) selecting the synergy matrix and mean vector corresponding to the desired grasp type.

## III. EXPERIMENTAL SETUP

In this section we describe in more detail the robot hands, the data acquisition system and experimental protocol used in the experiments.

### A. The Shadow Robot Hand

The *Shadow C5 air-muscle hand* closely matches the size and shape of a human hand and provides a total of 24 degrees-of-freedom, with 4 degrees-of-freedom per finger and 5 degrees-of-freedom for the thumb, as well as 2 degrees-of-freedom for the wrist and 1 degree-of-freedom for palm flexure[2]. See Fig. 1 for a photo of the hand and the kinematics diagram. The distal phalanges of the fingers are under-actuated from the medial joints, resulting in a total of 20 degrees-of-freedom controllable. All joints are tendon-driven and the tendons on the C5-type hand are actuated by a pair of McKibben-style air-muscles for each controllable joint. The muscles are elastic and provide full passive compliance, resulting in good grasp stability for a large variety of static grasp poses. The newer C6-type hand has the same mechanical structure, but the tendons are driven by electric motors, resulting in faster actuation.

### B. The iCub Hand

The iCub is a robot baby based on an 18 month to 2.5 year old child developed in the EU funded project RobotCub [13]. The iCub hands have a total of 19 degrees-of-freedom (excluding wrist) but only 9 actuators. By careful design of the coupled joints the dexterity of the hand was maximised while keeping the actuators to a minimum [14]. Thumb, index, ring and middle fingers have 4 joints: metacarpal, proximal, medial and distal phalanxes. The middle finger lacks the metacarpal joint because its adduction/abduction is less significant than the other fingers. There are 9 motors in each hand: 3 for the thumb, 2 for the index, 2 for the middle finger, 1 for the adduction/abduction and 1 for the coupled ring and little fingers. A photograph of the hand of the ISR–Lisbon iCub is shown in Fig. 2.

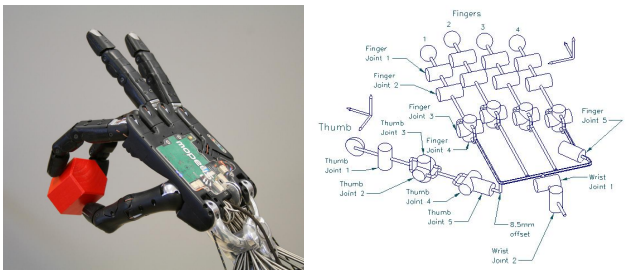


Fig. 1. The Shadow hand at Hamburg University.

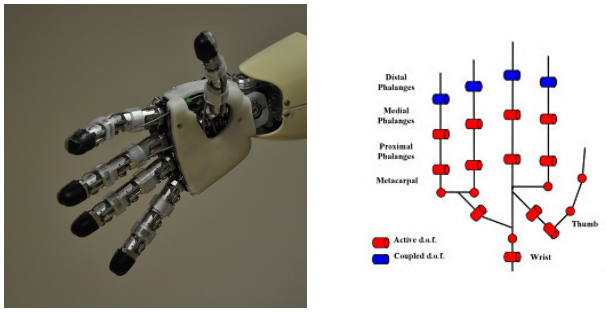


Fig. 2. The hand of the iCub at ISR–Lisboa.

### C. Teleoperation

In principle, any means to control the robot hand can be used to perform the grasps required for the extraction of the grasp synergies. However, direct tele-operation of the robot from a calibrated data-glove has proven to be the most efficient way to perform the experiments, because this approach exploits the experience of the humans (and their own grasp synergies).

The Immersion *CyberGlove-II* data-glove [3] is used to tele-operate the Shadow and the iCub hands for the experiments.

The *CyberGlove-II* provides a total of 22 sensors, with three flexure sensors per finger, three abduction sensors placed between the fingers, and one palm-flexure sensor. Four sensors measure the thumb position, and two sensors are provided for the wrist. The glove may be considered the benchmark input-device for recording human hand pose.

Due to the different sensor layout and sensor resolution, as well as different robot hand kinematics, a mapping is required to translate from the CyberGlove sensor values to the corresponding hand joint angles. Even for a single test-person, a slightly different fit of the glove will result in

[2]Shadow Robot Dexterous Hand, www.shadowrobot.com

[3]Cyberglove systems, www.cyberglovesystems.com

differing measured joint angles between different experiment runs. A calibration procedure is run for every test-person but still the mapping is not perfect. Calibrations errors must be compensated actively by the test-persons while controlling the actual robot hands on executing the grasps.

### D. The Protocol

For the recordings targeting the postural synergies, we used a set of twelve prototype objects. Given that most objects can be grasped at different parts (side, top, etc.) corresponding to different hand apertures, we defined 20 possible grasp postures as defined in table 4. See Fig. 3 for a photo of all objects together. The objects include three basic shapes (sphere, cylinder, box), different object diameters matched to typical human grasping tasks, and different materials (sponge, rubber, wood, metal).


Fig. 3. The set of prototype objects for grasping. The objects include three basic shapes (sphere, cylinder, box), different object diameters matched to typical human grasping tasks, and different materials (sponge, rubber, wood, metal).

We decided to record grasps for eight precision-grasp classes from the grasp taxonomy. These are *tripod*, *palmar pinch*, *lateral*, *writing tripod*, *parallel-extension*, *adduction-grip*, *tip pinch*, and *lateral tripod*, and are illustrated in Fig. 5.

| object name and grasp pose | width | height | length | material |
|---|---|---|---|---|
| big green ball | **86** | **86** | **86** | sponge |
| medium green ball | **64** | **64** | **64** | rubber |
| small white ball | **54** | **54** | **54** | sponge |
| big red cylinder, top | **64** | 76 | 76 | metal |
| big red cylinder, side | 64 | **76** | **76** | metal |
| medium green cylinder, top | **38** | 38 | 38 | sponge |
| medium green cylinder, side | 38 | **38** | **38** | sponge |
| small red cylinder, top | **59** | 27 | 27 | wood |
| small red cylinder, side | 59 | **27** | **27** | wood |
| pen, side | 150 | **12** | **12** | metal |
| small purple cube | **30** | **30** | **30** | wood |
| large blue box, long side | **77** | 39 | 39 | sponge |
| large blue box, short side | 77 | **39** | **39** | sponge |
| medium orange box, long side | **60** | 30 | 30 | wood |
| medium orange box, short side | 60 | **30** | **30** | wood |
| small red box, long side | **60** | 14 | 29 | wood |
| small red box, short side | 60 | **14** | 29 | wood |
| small red box, medium side | 60 | 14 | **29** | wood |
| large yellow box, short side | 80 | 80 | **38** | sponge |
| large yellow box, long side | **80** | **80** | 38 | sponge |

Fig. 4. Attributes of the prototype objects from the IST object set used for the recordings. Values in bold indicate the object dimensions along which opposition forces are applied. Dimensions are in millimetres.

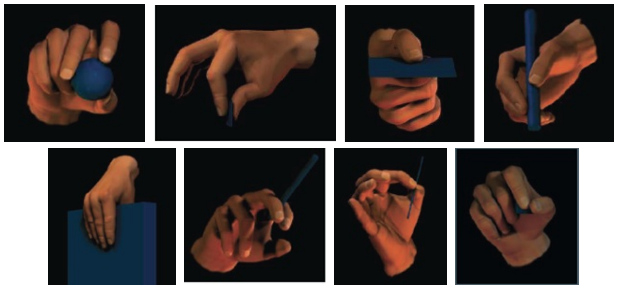

Fig. 5. The precision grasp types selected for the experiments: tripod, palmar pinch, lateral, writing tripod, parallel extension, adduction grip, lateral tripod.

| grasp type | per subject | on Shadow | on iCub |
|---|---|---|---|
| tripod | 20 | 80 | 100 |
| palmar pinch | 20 | 80 | 100 |
| lateral | 12 | 48 | 60 |
| writing tripod | 3 | 12 | 15 |
| parallel extension | 14 | 56 | 70 |
| adduction grip | 3 | 12 | 15 |
| tip pinch | 20 | 80 | 100 |
| lateral tripod | 15 | 60 | 75 |
| all | 107 | 428 | 535 |

Fig. 6. Number of grasp trials of a certain type performed by each test-person

The pinch and tripod grasps were selected because of their focus on manipulability of the target objects, while adduction-grip tests the abduction-joints of the Shadow and iCub hands.

During the experiments, the objects were presented to the test-persons in a fixed order (spheres first, then cylinders and boxes), but only for those grasps that were possible given the hand kinematics, or useful given the task. For the tripod, palmar pinch and tip-pinch, all object configurations were feasible. However, the lateral, lateral tripod and parallel extension grips were not feasible on the configurations requiring a large distance between the contact points. Also the writing tripod and adduction grip only make sense for configurations with a short distance between the contact points. Data collection on the Shadow hand involved 4 persons while on the iCub hand we had 5 subjects. Table 6 shows the number of trials of each grasp type performed by each test-person and overall in the Shadow hand and iCub hand datasets.

## IV. RESULTS

In this section we present the results or our analysis. Fig. 7 show the mean value of the different grasp types generated in the Shadow hand simulator.

The core result of the work is the analysis of the eigen-grasps for the different precision grasp types tested. First we show the amount of variance explained by an increasing number of synergies in the Shadow hand (Fig. 8) and the iCub hand (Fig. 9), for all the analysed grasp types. We can see that most of the variance is concentrated in the first few synergies. Looking at the $90\%$ variance line, which corresponds to mean square approximation errors below $10\%$, we

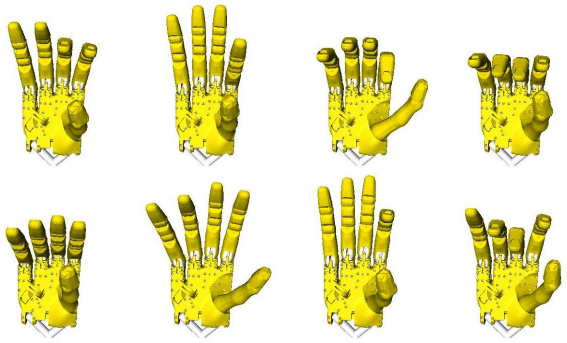

Fig. 7. Grasp poses corresponding to the origin of eigenspace for the eight reconstructed precision grasps: *tripod*, *palmar pinch*, *lateral*, *writing tripod*, *parallel extension*, *adduction grip*, *tip pinch*, and *lateral tripod*.

can observe that the Shadow hand requires 6 synergies to approximate the most complex grasp type, whereas for the iCub 5 synergies are sufficient. This is probably related to the fact that the thumb has a bigger dexterity in the Shadow Hand and thus plays a more active role in the grasping actions. For the adduction grip type, due to its simplicity, we can achieve the same low approximation errors with only the first two principal components.

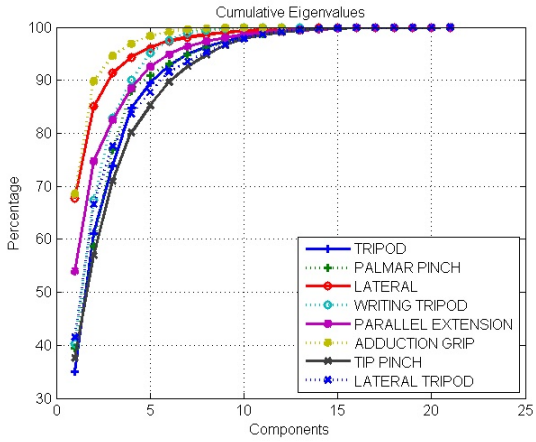


Fig. 8. The accumulated amplitude of the eigenvalues, in percentage, for the Shadow hand. 6 principal components are enough to explain 90% of the grasp variance.

Second we analyse the role of each of the synergies in the control of the robot hands. We do this by generating grasp postures by varying a single synergy coefficient $\alpha_m$ at each trial while keeping the others at zero (see Eq. (1)). Despite the ordering is arbitrary for each grasp type, we have found that the synergies related to hand closure is among the top two synergies. We can also find synergies that are related to in-hand translations and rotations of the manipulated objects. Figures 10 and 11 illustrate some of these synergies for the iCub and Shadow hands respectively, with and without manipulated objects. We observed that the activation of single synergies while the robot is grasping an object often leads to meaningful manipulation actions. Provided that a lower control ensures the fingers do not loose contact with the object while changing the synergy parameter, this fact

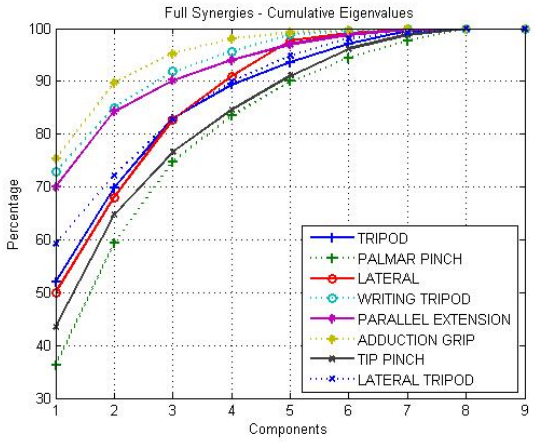


Fig. 9. The accumulated amplitude of the eigenvalues, in percentage, for the iCub hand. 5 principal components are enough to explain 90% of the grasp variance.

can be used to devise synergy based in-hand manipulation planning algorithms. The accompanying video shows some cases where the activation of single synergies is sufficient to perform simple in-hand movements while holding objects.

## V. CONCLUSIONS

We have derived synergy subspaces for 8 types of human like precision grasps, using principal component analysis on a large dataset of grasp trials. The synergies are represented in robot joint angle space, thus allowing for direct application in grasp planning and control. This was achieved by acquiring grasp data directly from the robot joint angles while they were tele operated by human subjects on performing grasp tasks on real objects. The analysis of the considered precision grips is coherent with previous works that also analysed grasp synergies: grasp tasks can be represented with low dimension linear subspaces embedded on the original joint angle space. According to our results, 5 and 6 dimensions, respectively for the iCub and Shadow robot hands, are sufficient to reconstruct with mean squared error lower than 10% all precision grasps considered in this work. From our analysis we also observed that individual synergies most often result in meaningful hand functions for the purpose of grasping and manipulation. Our future work will analyse this fact in more depth, in order to design in-hand manipulation planning algorithms that can take advantage of the low-dimensionality provided by grasp synergies.

## REFERENCES


[1] C. Ferrari and J. Canny, "Planning optimal grasps," in *Proc. IEEE International Conference on Robotics and Automation (ICRA'92)*, Nice, France, June 1992, pp. 2290–2295.

[2] K. Shimoga, "Robot grasp synthesis algorithms: a survey," *International Journal of Robotics Research*, vol. 15, no. 3, pp. 230–266, June 1996.

[3] A. Bicchi and V. Kumar, "Robotic grasping and contact: A review," in *Proc. IEEE International Conference on Robotics and Automation (ICRA'00)*, San Francisco, CA, US, Apr. 2000, pp. 348–353.

[4] M. Cutkosky, "On grasp choice, grasp models, and the design of hands for manufacturing tasks," *IEEE Transactions on Robotics and Automation*, vol. 5, no. 3, pp. 269–279, June 1989.

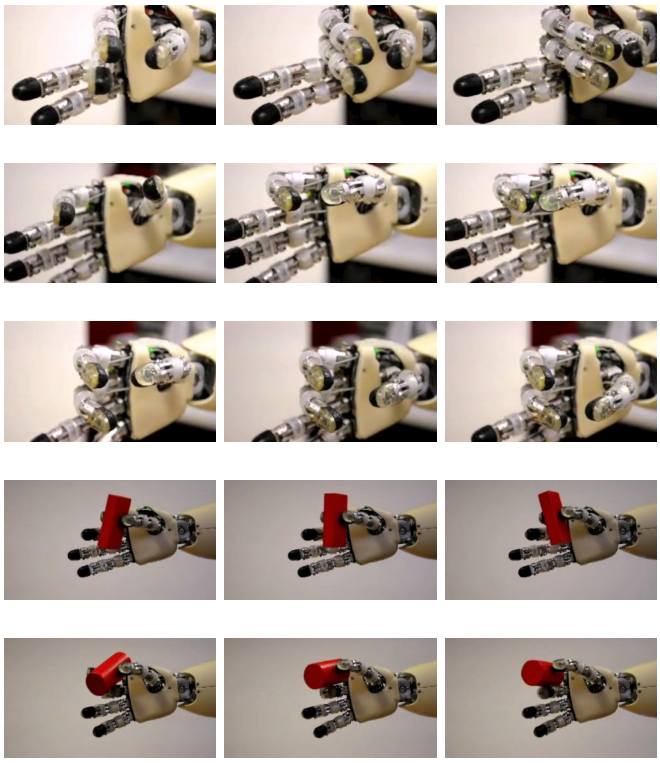

Fig. 10. In-hand synergies on the iCub hand. From top to bottom: parallel-extension translation; tip-pinch closure; tripod rotation; palmar-pinch rotation; writing-tripod rotation.

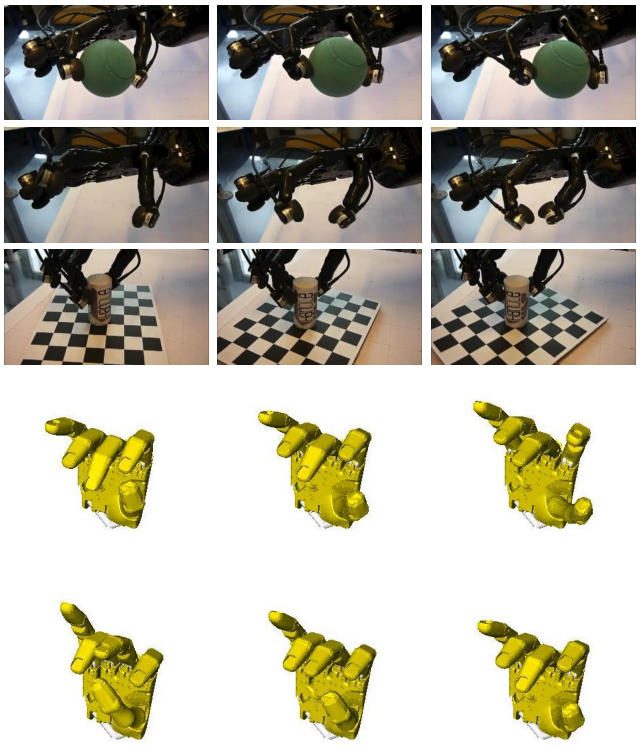

Fig. 11. In-hand synergies on the Shadow hand. From top to bottom: tip-pinch translation; tip-pinch closure; tripod rotation; tripod closure (simulation) and tripod rotation (simulation).


[5] T. Iberall, "Human prehension and dexterous robot hands," *International Journal of Robotics Research*, vol. 16, no. 3, pp. 285–299, June 1997.

[6] M. Kondo, J. Ueda, and T. Ogasawara, "Recognition of in-hand manipulation using contact state transition for multifingered robot hand control," *Robotics and Autonomous Systems*, vol. 56, no. 1, pp. 66–81, Jan. 2008.

[7] M. Santello, M. Flanders, and J. F. Soechting, "Postural hand synergies for tool use," *Journal of Neuroscience*, vol. 18, no. 23, pp. 10 105–10 115, Dec. 1998.

[8] M. Ciocarlie, C. Goldfeder, and P. K. Allen, "Dimensionality reduction for hand-independent dexterous robotic grasping," in *Proc. IEEE International Conference on Intelligent Robots and Systems (IROS'07)*, San Diego, CA, US, Oct. 2007, pp. 3270–3275.

[9] M. Ciocarlie and P. K. Allen, "Hand posture subspaces for dexterous robotic grasping," *International Journal of Robotics Research*, vol. 28, no. 7, pp. 851–866, July 2009.

[10] A. Miller and P. Allen, "Graspit! a versatile simulator for robotic grasping," *IEEE Robotics and Automation Magazine*, vol. 11, no. 4, pp. 110–122, Dec. 2004.

[11] C. Goldfeder, M. Ciocarlie, H. Dang, and P. K. Allen, "The columbia grasp database," in *Proc. IEEE International Conference on Robotics and Automation (ICRA'09)*, Kobe, Japan, May 2009, pp. 1710–1716.

[12] T. Feix, H. bodo Schmiedmayer, J. Romero, and D. Kragić, "A comprehensive grasp taxonomy," in *Proc. of Robotics, Science and Systems Workshop on Understanding the Human Hand for Advancing Robotic Manipulation*, 2009.

[13] N. G. Tsagarakis, G. Metta, G. Sandini, D. Vernon, R. Beira, F. Becchi, L. Righetti, J. Santos-Victor, a. J. Ijspeert, M. C. Carrozza, and D. G. Caldwell, "icub: the design and realization of an open humanoid platform for cognitive and neuroscience research," *Advanced Robotics*, vol. 21, no. 10, pp. 1151–1175, Jan. 2007.

[14] S. Davis, N. Tsagarakis, and D. G. Caldwell, "The initial design and manufacturing process of a low cost hand for the robot icub," in *Proc. IEEE International Conference on Humanoid Robots (Humanoids'08)*, Daejeon, South Korea, Dec. 2008, pp. 40–45.